Chiral symmetry breaking in (2+1)-dimensional Gross-Neveu model with Zeeman interaction with external tilted magnetic field.

Р. Н. Жохов

6 ноября 2013 г.

Model

- In spatially three-dimensional space some physical system is constraint by a two-dimensional plane which is perpendicular to the $\hat{z}$ coordinate axis.
- There is an external homogeneous and time independent magnetic field $\vec{B}$ tilted with respect to this plane.
  The corresponding (3+1)-dimensional vector potential A_μ is given by $A_{0,1} = 0$, $A_2 = B_\perp x$, $A_3 = B_\parallel y$, i.e. $B_x = B_\parallel$, $B_y = 0$, $B_z = B_\perp$.
- The plane physical system consists of quasi-particles (electrons) with two spin projections, $\pm 1/2$, on the direction of the magnetic field $\vec{B}$. (The Zeeman interaction of electron magnetic moment with $\vec{B}$).
- Their low-energy dynamics is described by the (2+1)-dimensional Gross-Neveu type Lagrangian.

Lagrangian

$$L = \sum_{k=1}^{2} \bar{\psi}_{ka} \left[\gamma^0 i\partial_t + \gamma^1 i\nabla_1 + \gamma^2 i\nabla_2 - \nu(-1)^k \gamma^0 \right] \psi_{ka} + \frac{G}{N} \left(\sum_{k=1}^{2} \bar{\psi}_{ka} \psi_{ka} \right)$$

where $\nabla_{1,2} = \partial_{1,2} + ieA_{1,2}$, index $a = 1, ..., N$ of the internal $O(N)$ group.

$\psi_{ka}(x)$ - the massless Dirac fermion field, transforming over a reducible 4-component spinor representation of the (2+1)-dimensional Lorentz group.

$k = 1, 2$: spinor fields $\psi_{1a}(x)$ and $\psi_{2a}(x)$ $(a = 1, ..., N)$ correspond to electrons with spin projections 1/2 and -1/2 on the direction of external magnetic field.

$\nu = g_L \mu_B |\vec{B}|/2$, where $|\vec{B}| = \sqrt{B_{\parallel}^2 + B_{\perp}^2}$, g_L is the spectroscopic Lande factor and μ_B is the Bohr magneton.

γ-matrices

$$\tilde{\gamma}^0 = \sigma_3 = \begin{pmatrix} 1 & 0 \\ 0 & -1 \end{pmatrix}, \; \tilde{\gamma}^1 = i\sigma_1 = \begin{pmatrix} 0 & i \\ i & 0 \end{pmatrix}, \; \tilde{\gamma}^2 = i\sigma_2 = \begin{pmatrix} 0 & 1 \\ -1 & 0 \end{pmatrix}$$

$$\gamma^\mu = \begin{pmatrix} \tilde{\gamma}^\mu & 0 \\ 0 & -\tilde{\gamma}^\mu \end{pmatrix}.$$

Chiral symmetry

The model is invariant under the discrete chiral transformation,

$$\psi_{ka} \rightarrow \gamma^5 \psi_{ka}$$

Auxiliary Lagrangian

Auxiliary Lagrangian

$$\mathcal{L} = -\frac{N\sigma^2}{4G} + \sum_{k=1}^{2} \bar{\psi}_{ka}\Big(\gamma^0 i\partial_t + \gamma^1 i\nabla_1 + \gamma^2 i\nabla_2 + \mu_k\gamma^0 - \sigma\Big)\psi_{ka},$$

where $\mu_1 = \nu$, $\mu_2 = -\nu$ and from now on $\nu = \mu_B|\vec{B}|$

Auxiliary Lagrangian

Auxiliary Lagrangian

$$\mathcal{L} = -\frac{N\sigma^2}{4G} + \sum_{k=1}^{2} \bar{\psi}_{ka}\Big(\gamma^0 i\partial_t + \gamma^1 i\nabla_1 + \gamma^2 i\nabla_2 + \mu_k\gamma^0 - \sigma\Big)\psi_{ka},$$

where $\mu_1 = \nu$, $\mu_2 = -\nu$ and from now on $\nu = \mu_B|\vec{B}|$
Equation of motion for field $\sigma(x)$

$$\sigma(x) = -\frac{2G}{N}\sum_{k=1}^{2} \bar{\psi}_{ka}\psi_{ka}.$$

In the leading order of the large-N approximation, the effective action $\mathcal{S}_{\text{eff}}(\sigma)$

$$\exp(i\mathcal{S}_{\text{eff}}(\sigma)) = \int \prod_{k=1}^{2} \prod_{a=1}^{N} [d\bar{\psi}_{ka}][d\psi_{ka}] \exp\Big(i \int \mathcal{L}\, d^3x\Big),$$

where

$$\mathcal{S}_{\text{eff}}(\sigma) = -\int d^3x \frac{N}{4G}\sigma^2(x) + \widetilde{\mathcal{S}}_{\text{eff}}.$$

The fermion contribution to the effective action, i.e. the term $\widetilde{\mathcal{S}}_{\text{eff}}$, is given by

$$\exp(i\widetilde{\mathcal{S}}_{\text{eff}}) = \int \prod_{l=1}^{2} \prod_{a=1}^{N} [d\bar{\psi}_{la}][d\psi_{la}] \exp\Big\{ i \int \sum_{k=1}^{2} \bar{\psi}_{ka} \Big(\gamma^0 i\partial_t +$$

$$+\gamma^1 i\nabla_1 + \gamma^2 i\nabla_2 + \mu_k \gamma^0 - \sigma \Big) \psi_{ka} d^3x \Big\}.$$

Effective potential

The ground state expectation value $\langle \sigma(x) \rangle$ is determined by the equation,

$$\frac{\delta \mathcal{S}_{\text{eff}}}{\delta \sigma(x)} = 0.$$

Effective potential

The ground state expectation value $\langle\sigma(x)\rangle$ is determined by the equation,

$$\frac{\delta\mathcal{S}_{\text{eff}}}{\delta\sigma(x)} = 0.$$

For simplicity we suppose that the ground state expectation value does not depend on space-time coordinates, i.e.

$$\langle\sigma(x)\rangle \equiv M,$$

where M is a constant quantity.

Effective potential

The ground state expectation value $\langle\sigma(x)\rangle$ is determined by the equation,

$$\frac{\delta\mathcal{S}_{\text{eff}}}{\delta\sigma(x)} = 0.$$

For simplicity we suppose that the ground state expectation value does not depend on space-time coordinates, i.e.

$$\langle\sigma(x)\rangle \equiv M,$$

where M is a constant quantity.
In fact, it is a coordinate of the global minimum point of the thermodynamic potential (TDP) $\Omega(M;\nu,B_\perp)$. In the leading order of the large-N expansion the TDP is defined by the following expression:

$$\int d^3x\Omega(M;\nu,B_\perp) = -\frac{1}{N}\mathcal{S}_{\text{eff}}(\sigma(x))\Big|_{\sigma(x)=M},$$

$$\int d^3x \Omega(M;\nu,B_\perp) =$$

$$\int d^3x \frac{M^2}{4G} + \frac{i}{N} \ln \left(\int \prod_{l=1}^{2} \prod_{b=1}^{N} [d\bar{\psi}_{lb}][d\psi_{lb}] \exp \left(i \int \sum_{k=1}^{2} \bar{\psi}_{ka} D_k \psi_{ka} d^3x \right) \right),$$

where $D_k = \gamma^0 i\partial_t + \gamma^1 i\nabla_1 + \gamma^2 i\nabla_2 + \mu_k \gamma^0 - M$.

$$\Omega^{ren}(M;\nu,B_\perp) = \Omega^{ren}(M;B_\perp) - \frac{eB_\perp}{\pi}\sum_{n=0}^{\infty} s_n\theta(\nu-\varepsilon_n)(\nu-\varepsilon_n),$$

$$\Omega^{ren}(M;\nu,B_\perp) = \Omega^{ren}(M;B_\perp) - \frac{eB_\perp}{\pi}\sum_{n=0}^{\infty} s_n\theta(\nu-\varepsilon_n)(\nu-\varepsilon_n),$$

$$\Omega^{ren}(M;B_\perp) = \frac{M^2}{\pi g} + \frac{MeB_\perp}{\pi} - \frac{(2eB_\perp)^{3/2}}{\pi}\zeta\left(-\frac{1}{2},\frac{M^2}{2eB_\perp}\right),$$

$$\Omega^{ren}(M;\nu,B_\perp) = \Omega^{ren}(M;B_\perp) - \frac{eB_\perp}{\pi}\sum_{n=0}^{\infty} s_n\theta(\nu-\varepsilon_n)(\nu-\varepsilon_n),$$

$$\Omega^{ren}(M;B_\perp) = \frac{M^2}{\pi g} + \frac{MeB_\perp}{\pi} - \frac{(2eB_\perp)^{3/2}}{\pi}\zeta\left(-\frac{1}{2},\frac{M^2}{2eB_\perp}\right),$$

$$\left.\frac{\partial\Omega^{ren}(M;B_\perp)}{\partial M}\right|_{M\to 0_+} = -\frac{eB_\perp}{\pi},$$

$$\Omega^{un}(M;\nu) = \frac{M^2}{4G} - 2\int \frac{d^2p}{(2\pi)^2}\,(2E) - 2\int \frac{d^2p}{(2\pi)^2}\Big(|E+\nu|+|E-\nu|-2E\Big).$$

$$\Omega^{un}(M;\nu) = \frac{M^2}{4G} - 2\int \frac{d^2p}{(2\pi)^2}\,(2E) - 2\int \frac{d^2p}{(2\pi)^2}\Big(|E+\nu|+|E-\nu|-2E\Big).$$

$$\Omega^{ren}(M;\nu) = \lim_{\Lambda\to\infty}\left\{\Omega^{reg}(M;\nu)\Big|_{G=G(\Lambda)} + \frac{4\Lambda^3(\sqrt{2}+\ln(1+\sqrt{2}))}{3\pi^2}\right\}.$$

$$\Omega^{un}(M;\nu) = \frac{M^2}{4G} - 2\int \frac{d^2p}{(2\pi)^2}\,(2E) - 2\int \frac{d^2p}{(2\pi)^2}\Big(|E+\nu|+|E-\nu|-2E\Big).$$

$$\Omega^{ren}(M;\nu) = \lim_{\Lambda\to\infty}\left\{\Omega^{reg}(M;\nu)\Big|_{G=G(\Lambda)} + \frac{4\Lambda^3(\sqrt{2}+\ln(1+\sqrt{2}))}{3\pi^2}\right\}.$$

$$V(M) \equiv \Omega^{ren}(M;\nu)\Big|_{\nu=0} = \frac{M^2}{\pi g} + \frac{2M^3}{3\pi}.$$

$$\Omega^{un}(M;\nu) = \frac{M^2}{4G} - 2\int \frac{d^2p}{(2\pi)^2}\,(2E) - 2\int \frac{d^2p}{(2\pi)^2}\Big(|E+\nu|+|E-\nu|-2E\Big).$$

$$\Omega^{ren}(M;\nu) = \lim_{\Lambda\to\infty}\left\{\Omega^{reg}(M;\nu)\Big|_{G=G(\Lambda)} + \frac{4\Lambda^3(\sqrt{2}+\ln(1+\sqrt{2}))}{3\pi^2}\right\}.$$

$$V(M) \equiv \Omega^{ren}(M;\nu)\Big|_{\nu=0} = \frac{M^2}{\pi g} + \frac{2M^3}{3\pi}.$$

$$\frac{1}{4G} \equiv \frac{1}{4G(\Lambda)} = \frac{4\Lambda\ln(1+\sqrt{2})}{\pi^2} + \frac{1}{\pi g} \equiv \frac{1}{4G_c} + \frac{1}{\pi g},$$

where g is a finite and Λ-independent model parameter with dimensionality of inverse mass and $G_c = \frac{\pi^2}{16\Lambda\ln(1+\sqrt{2})}$.

The case $g > 0$, $B_{\|} = 0$, i.e. $B_{\perp} = |\vec{B}|$

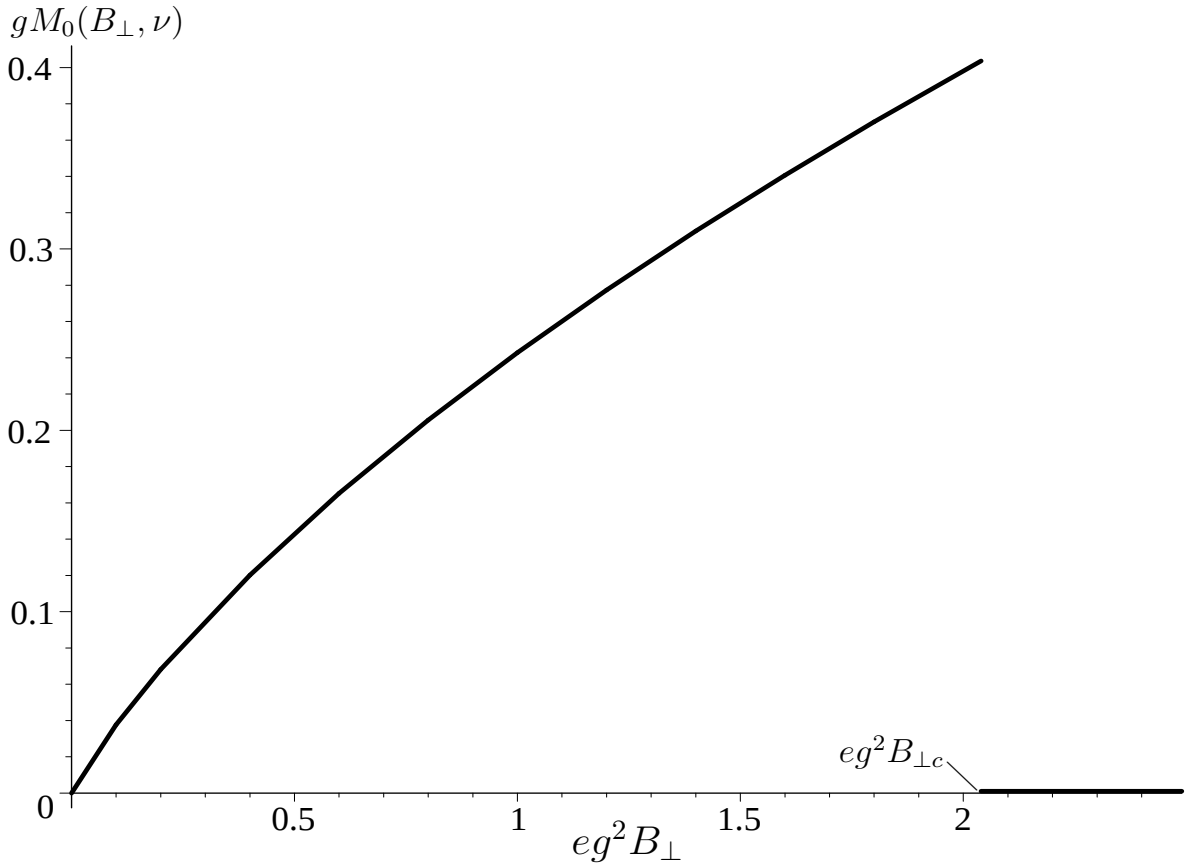

Рис.: The mass gap $M_0(B_\perp, \nu)$ vs $B_\perp$ in the particular case $B_{\|} = 0$ and $g = 5g_c \equiv 10\mu_B/e$.
The gap is an increasing function vs $B_\perp$ up to a critical value $B_{\perp c}$, where it vanishes sharply, i.e. the first order phase transition occurs.

The case $g > 0$, The case $B_\perp \neq |\vec{B}|$.

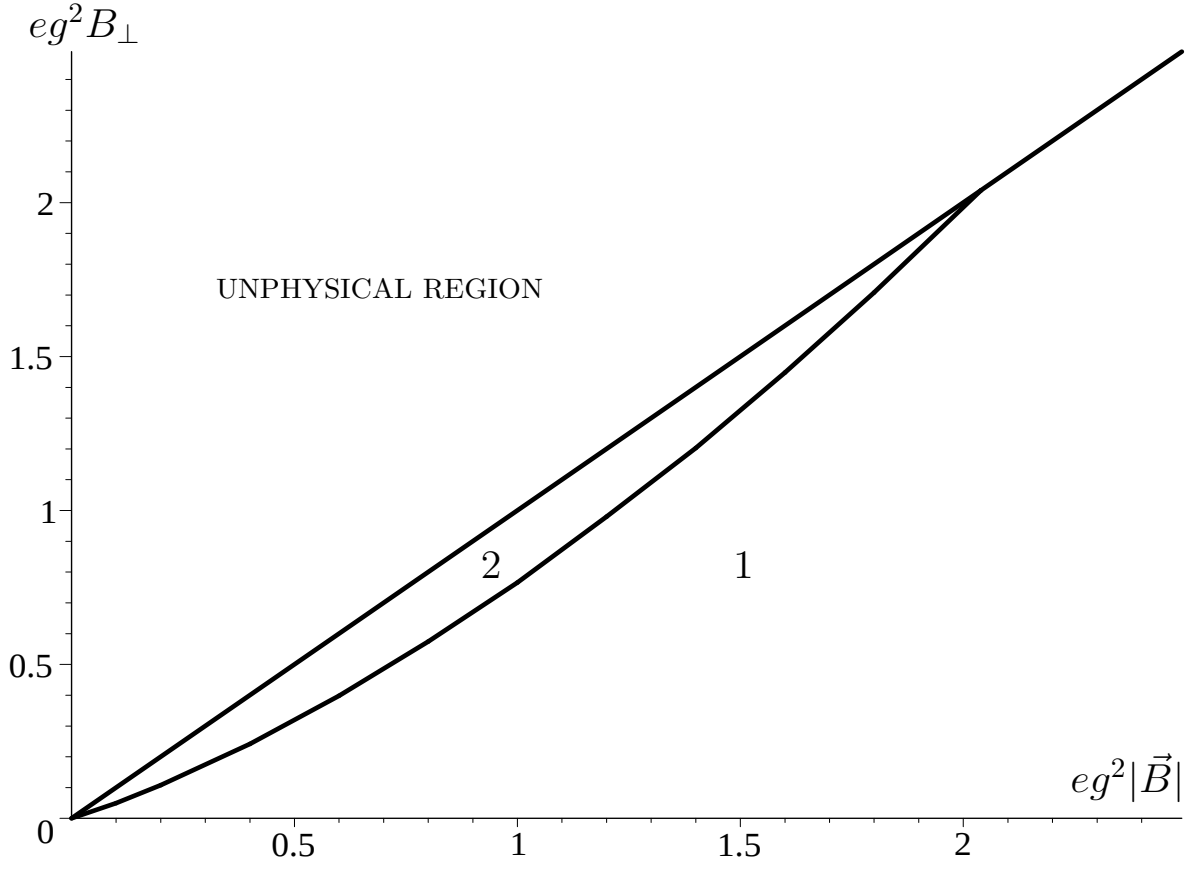

Рис.: The $(|\vec{B}|, B_\perp)$-phase portrait of the model at $g = 5g_c \equiv 10\mu_B/e$. The numbers 1 and 2 denote the chirally symmetric and chirally broken phases, respectively. In the unphysical region $B_\perp > |\vec{B}|$. The boundary between 1 and 2 phases is the curve of the first order phase transitions.

Magnetization

$$m(|\vec{B}|, B_\perp) \equiv -\frac{d\Omega^{ren}(M;\nu,B_\perp)}{d|\vec{B}|}\Big|_{M=M_0(B_\perp,\nu)},$$

Magnetization

$$m(|\vec{B}|, B_\perp) \equiv -\frac{d\Omega^{ren}(M;\nu,B_\perp)}{d|\vec{B}|}\bigg|_{M=M_0(B_\perp,\nu)},$$

$$m(|\vec{B}|, B_\perp) = -\frac{B_\perp}{|\vec{B}|}\frac{\partial\Omega^{ren}(M;B_\perp)}{\partial B_\perp}\bigg|_{M=M_0(B_\perp,\nu)} +$$

$$\frac{eB_\perp}{\pi|\vec{B}|}\sum_{n=0}^{\infty} s_n\theta(\nu-\varepsilon_n)\left(2\nu-\frac{\varepsilon_n^2+enB_\perp}{\varepsilon_n}\right)\bigg|_{M=M_0(B_\perp,\nu)},$$

Magnetization

$$m(|\vec{B}|, B_\perp) \equiv -\frac{d\Omega^{ren}(M;\nu,B_\perp)}{d|\vec{B}|}\Big|_{M=M_0(B_\perp,\nu)},$$

$$m(|\vec{B}|, B_\perp) = -\frac{B_\perp}{|\vec{B}|}\frac{\partial\Omega^{ren}(M;B_\perp)}{\partial B_\perp}\Big|_{M=M_0(B_\perp,\nu)} +$$

$$\frac{eB_\perp}{\pi|\vec{B}|}\sum_{n=0}^{\infty} s_n\theta(\nu-\varepsilon_n)\left(2\nu-\frac{\varepsilon_n^2+enB_\perp}{\varepsilon_n}\right)\Big|_{M=M_0(B_\perp,\nu)},$$

$$m(|\vec{B}|, B_\perp)\Big|_{\text{phase 1}} = \frac{eB_\perp}{\pi}\left[\frac{3}{|\vec{B}|}\sqrt{2eB_\perp}\zeta(-1/2)+2\mu_B\right] +$$

$$+\frac{2eB_\perp}{\pi|\vec{B}|}\sum_{n=1}^{\infty}\theta(\nu-\sqrt{2enB_\perp})\left(2\nu-\frac{3}{2}\sqrt{2enB_\perp}\right),$$

Oscillations of the magnetization The case $g > 0$.

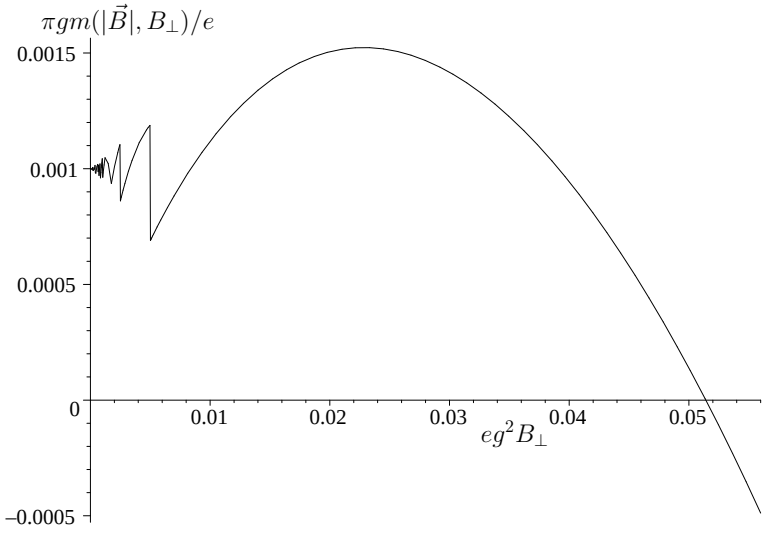

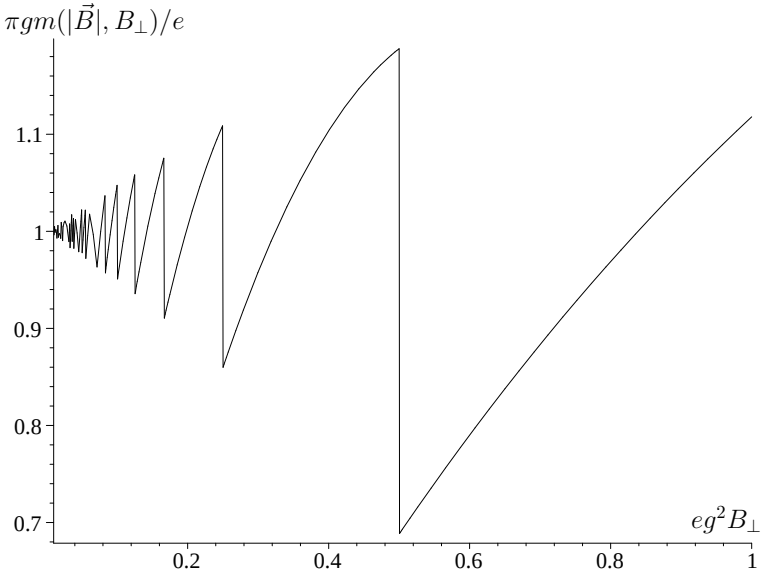

Рис.: Magnetization $m(|\vec{B}|, B_\perp)$ vs $B_\perp$ at fixed $eg^2|\vec{B}| = 1$ and $g = 5g_c \equiv 10\mu_B/e$.

Рис.: Magnetization $m(|\vec{B}|, B_\perp)$ vs $B_\perp$ at fixed $eg^2|\vec{B}| = 1$ and $g = 0.5g_c \equiv \mu_B/e$.

Magnetic oscillations usually occur in the presence of chemical potential μ. Magnetic oscillations can be induced even at $\mu = 0$ by tilting the external magnetic field with respect to a system plane.

The case $g < 0$, $B_{\|} = 0$, $|g| = \mu_B/e$.

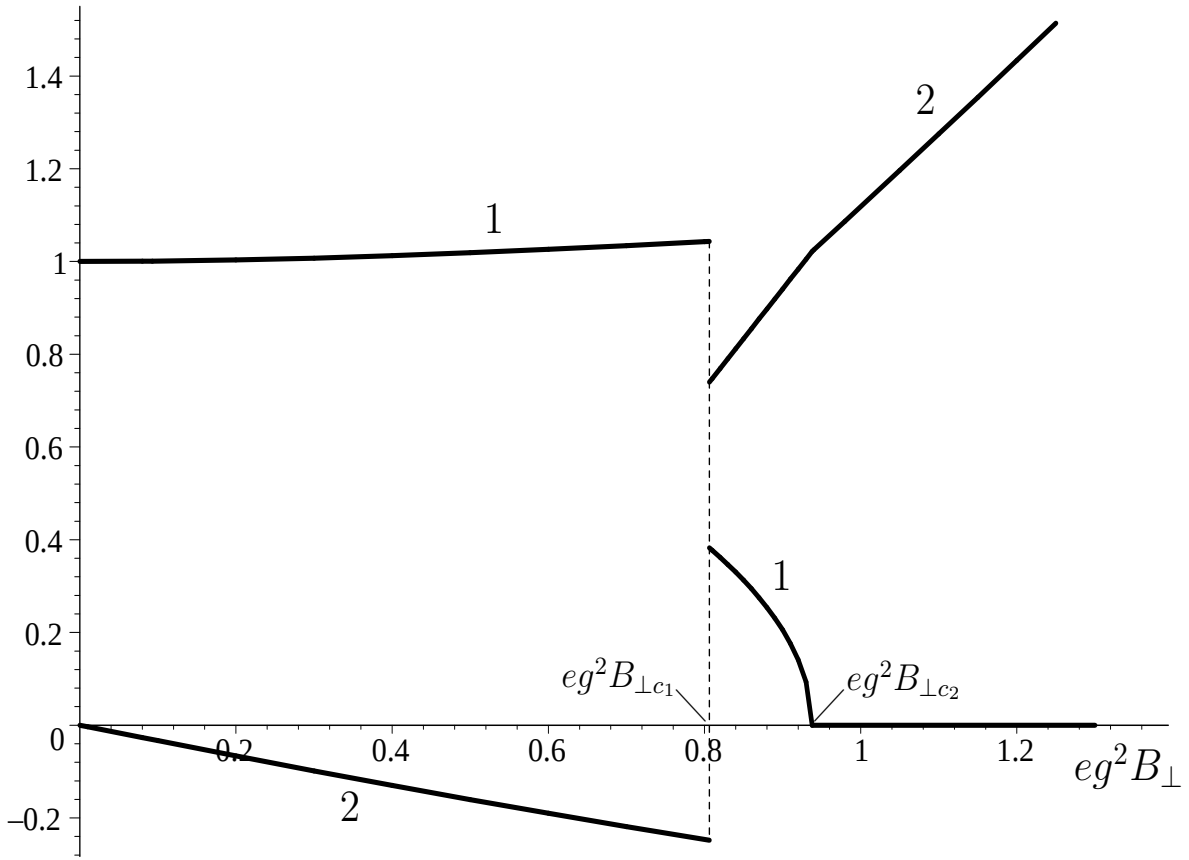

Рис.: Mass gap $M_0(B_\perp, \nu)$ and magnetization $m(|\vec{B}|, B_\perp)$ vs $B_\perp$ in the particular case $B_{\|} = 0$ and $|g| = \mu_B/e$. Curves 1 and 2 are the plots of the dimensionless quantities $gM_0(B_\perp, \nu)$ and $\pi g m(|\vec{B}|, B_\perp)/e$, correspondingly. Here $eg^2B_{\perp c_1} \approx 0.81$ and $eg^2B_{\perp c_2} \approx 0.94$.

The case $g < 0$, $B_{\parallel} \neq 0$, $|g| = \mu_B/e$.

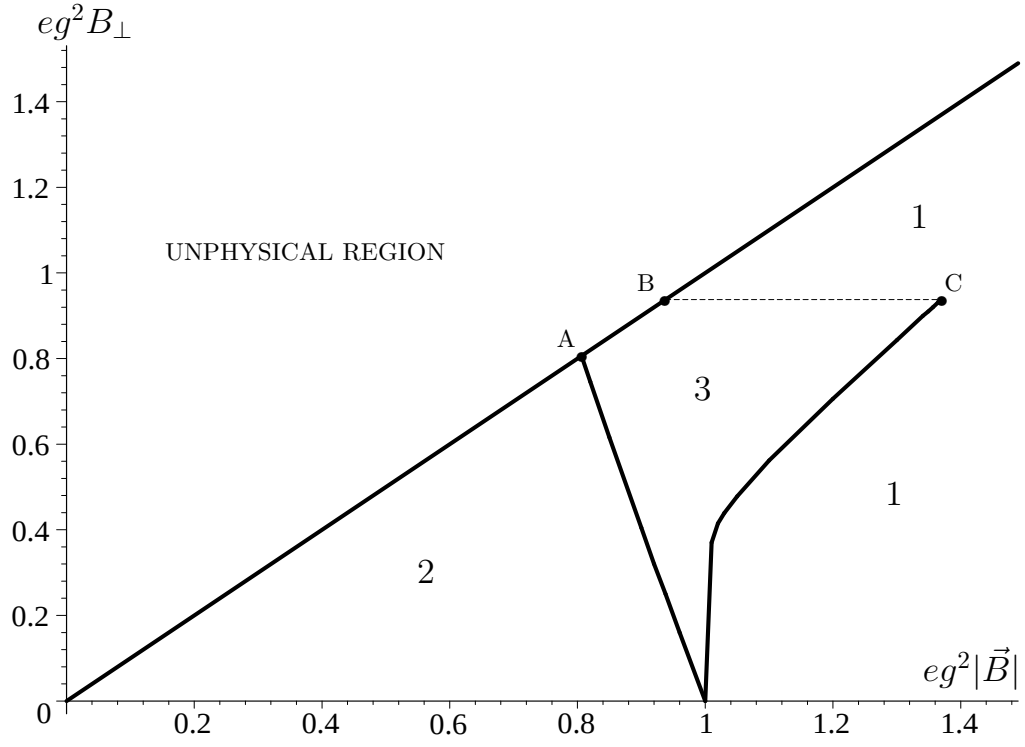

Рис.: The $(|\vec{B}|, B_\perp)$-phase portrait of the model at $|g| = \mu_B/e$. The numbers 1 denote the chirally symmetric phase, whereas the numbers 2 and 3 denote two different chirally broken phases (on the boundary between 2 and 3 the mass gap changes by a jump). The line BC is a curve of second order phase transitions; on the other lines the first order phase transitions take place. The unphysical region: $B_\perp > |\vec{B}|$.

The case $g < 0, |g| \neq \mu_B/e$.

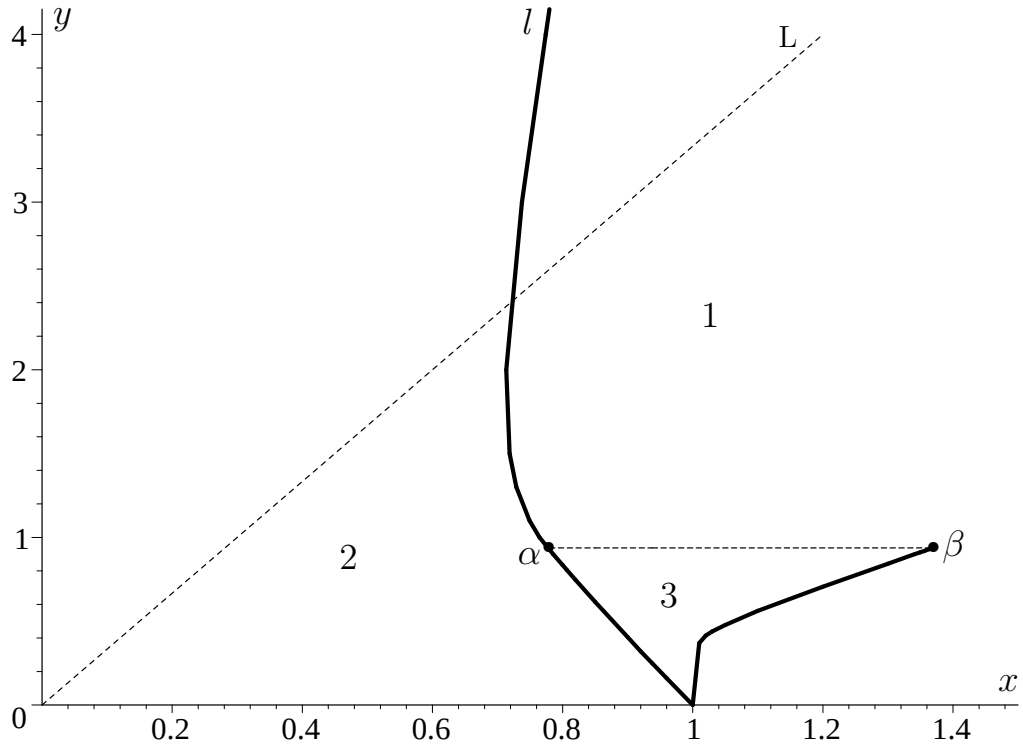

Рис.: The (x, y)-phase diagram of the model, where $x = \mu_B|\vec{B}||g|$ and $y = eg^2B_\perp$, typical for values of $c \equiv e|g|/\mu_B < c^* \approx 28$. Physical region of the diagram corresponding to $B_\perp \leq |\vec{B}|$ relation lies just below the line L=$\{(x, y) : \ y = cx\}$. (1-the chirally symmetric phase, 2,3 -two different chirally broken phases. First order phase transitions occur on the solid curves. On the line $\alpha\beta$ second order phase transitions take place.

The case $g < 0, |g| \neq \mu_B/e$.

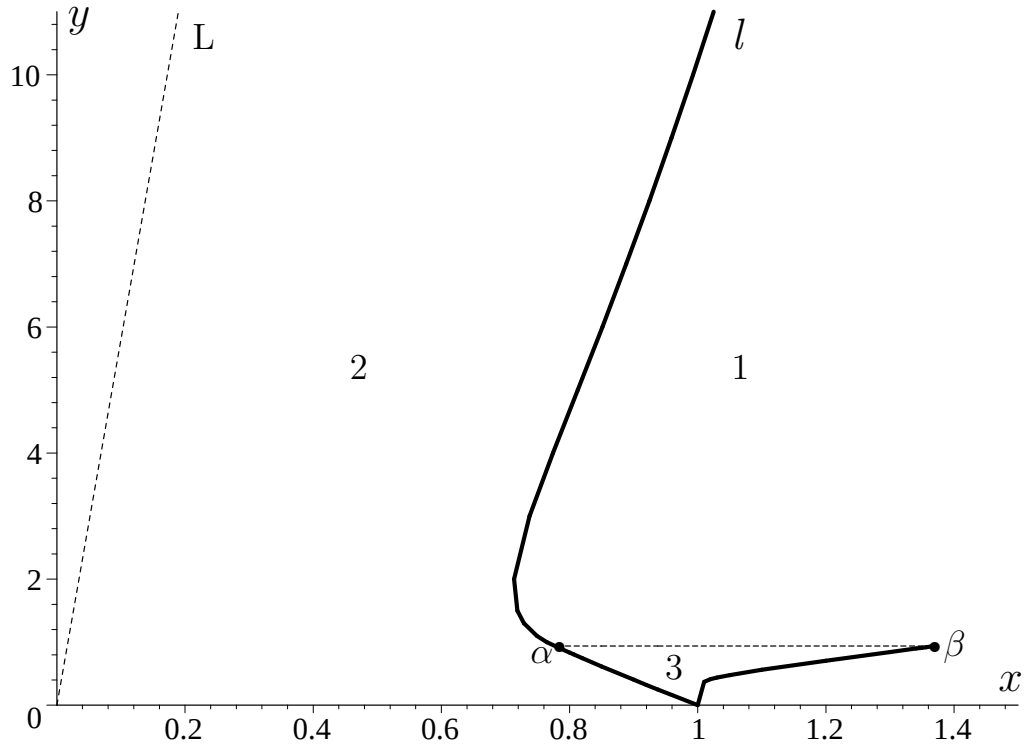

Рис.: The (x, y)-phase diagram of the model, where $x = \mu_B|\vec{B}||g|$ and $y = eg^2B_\perp$, typical for values of $c \equiv e|g|/\mu_B > c^* \approx 28$. Physical region of the diagram, corresponding to $B_\perp \leq |\vec{B}|$ relation, lies just below and/or to the right of the line L=$\{(x, y) : \ y = cx\}$. Other notations are the same as in the previous figure.

Numerical estimates in the context of condensed matter physics

In our numerical estimates we use the following relations : $\mu_B = e/(2m_e)$, where m_e is the electron rest mass, $m_e \approx 0.5$ MeV; 1 Tesla ≈ 700 eV^2; $e \approx 1/\sqrt{137}$, as in graphene.

- $g < 0$, $M_{0F} \equiv -v_F/g$, $x_F = x/v_F \equiv \mu_B|\vec{B}||g|/v_F$,
  In case $x_F = 1$ $|B_0| = v_F/(|g|\mu_B) = M_{0F}/\mu_B$.
  $M_{0F} = 1meV$: $|\vec{B}_0| \approx 14\,Teslas$.
  $M_{0F} = 10meV$: $|\vec{B}_0| \approx 140\,Teslas$.
  The magnitudes of $|\vec{B}|$, at which one can observe phase transitions, are even less and might be as small as $0.7|\vec{B}_0|$.
- If $v_F = 1/300$ and $g_S = 2$, as in graphene, then the slope factor c_F of the line L is approximately equal to 10^3 at $M_{0F} = 10$ meV, whereas it is of order of 10^4 at $M_{0F} = 1$ meV, i.e. $c_F \gg c^* \approx 28$.
  Hence, graphene-like planar systems corresponds to the case $c \equiv e|g|/\mu_B > c^* \approx 28$.

Numerical estimates in the context of condensed matter physics

- Chiral symmetry cannot be restored by an arbitrary strong external perpendicular magnetic field, and the enhancement effect is realized at $B_\perp \lessapprox |\vec{B}|$. However, tilting the magnetic field away from a normal of the plane, it is possible to restore the symmetry, if $|\vec{B}| > 0.7|\vec{B}_0|$. The angle φ_0 between $\vec{B}$ and the plane of the system, at which the restoration of the symmetry occurs.
  At $|\vec{B}| = 1.5|\vec{B}_0|$, $M_{0F} = 10$ meV $\sin\varphi_0 \approx 0.02$, $\sin\varphi_0 \approx 0.2$
  At $|\vec{B}| = 1.5|\vec{B}_0|$, $M_{0F} = 1$ meV $\sin\varphi_0 \approx 0.002$
  I.e. the restoration of the chiral symmetry occurs at very weak $B_\perp$-components of the magnetic field.

Numerical estimates in the context of condensed matter physics

- $g_S = 200$ and $v_F = 1/300$
  At $M_{0F} = 1$ meV, $|\vec{B}_0| = 0.14$ Teslas
  At $M_{0F} = 10$ meV, $|\vec{B}_0| = 1.4$ Teslas

We see that the effects which are due to the Zeeman interaction can be observed in real condensed matter systems at reasonable laboratory magnitudes of external magnetic fields.

Conclusions

- At $\mu_B \neq 0$ and $g > 0$, $g_c = 2\mu_B/e$,
  At $g > g_c$ an arbitrary rather weak external magnetic field $\vec{B}$ induces spontaneous chiral symmetry breaking provided that there is not too great a deviation of $\vec{B}$ from a vertical as well as that $|\vec{B}| < B_c(g)$, where $0 < B_c(g) < \infty$.
  At $0 < g < g_c$ chiral symmetry cannot be broken by an external magnetic field. (In contrast, at $\mu_B = 0$ and any values of $g > 0$ the chiral symmetry breaking is induced by arbitrary external magnetic field $\vec{B}$ such that $\vec{B}_\perp \neq 0$.)
- Suppose that $\mu_B \neq 0$, $g > g_c > 0$ and chiral symmetry is broken, i.e. $\vec{B}$ has a rather large $B_\perp$ component. Then chiral symmetry can be restored simply by tilting magnetic field to a system plane, i.e. without any increase of its modulus $|\vec{B}|$.

Conclusions

- We have shown that at $\mu_B \neq 0$, $g > 0$ and arbitrary fixed $|\vec{B}| \neq 0$ one can observe oscillations of the magnetization in the region of small values of $B_\perp$.
- At $\mu_B \neq 0$ and $g < 0$, at non-vanishing Zeeman interaction the phase portrait of the model contains at least two chirally nonsymmetric phases. In the phase 2, which is a diamagnetic one, the enhancement of the chiral symmetry is occurred, whereas in the paramagnetic phase 3 it is absent.
- At $g < 0$ and $c \equiv e|g|/\mu_B < c^* \approx 28$, sufficiently high values of $|\vec{B}|$ (even at a perpendicular magnetic field) restores the chiral symmetry.
  At $g < 0$ and $c \equiv e|g|/\mu_B > c^*$ the line L does not cross any of the critical curves of the figure. So, in this case at an arbitrary perpendicular magnetic field chiral symmetry cannot be restored. Tilting the magnetic field restores the symmetry. This situation is typical for graphene-like planar systems.

Спасибо за внимание

Спасибо за внимание!